Bubble Rearrangement Duration in Foams near the Jamming Point

Marie Le Merrer,[1] Sylvie Cohen-Addad,[1,2] and Reinhard Höhler[1,2]
[1]Université Paris 6, UMR 7588 CNRS-UPMC, INSP, 4 place Jussieu, 75252 Paris cedex 05, France
[2]Université Paris-Est, LPMDI, 5 boulevard Descartes, 77454 Marne-la-Vallée, France
(Received 29 December 2011; revised manuscript received 11 February 2012; published 2 May 2012)

We investigate the dynamics of bubble rearrangements in coarsening foams, using a time-resolved multiple light scattering technique. We measure the average duration of such events as a function of the foam confinement pressure. Rearrangements slow down as the pressure is decreased toward the jamming point. Our results are explained by a scaling law based on the balance of pressure and Darcy flow, highlighting an analogy between wet foams with mobile interfaces and suspensions of hard grains.

DOI: 10.1103/PhysRevLett.108.188301 PACS numbers: 47.57.Bc

Liquid foams are concentrated dispersions of gas bubbles in a surfactant solution. Driven by Laplace pressure differences, gas diffuses through the liquid from smaller to larger bubbles [1,2]; in order to minimize surface energy, the foam structure evolves through intermittent bubble rearrangements [3]. These coarsening-induced events govern the slow viscoelastic foam response [4,5], and similar rearrangements are the elementary processes of plastic flow [6]. The rearrangement duration thus appears as a key parameter to describe how the microstructure dynamics control the macroscopic rheological response. Investigations of event duration in foams of low liquid volume fraction (dry foams) [7,8] have shown that, in this case, dissipation at the liquid-gas interfaces is dominant and that the event duration is proportional to κ/γ, where κ is the dilational surface viscosity and γ is the liquid surface tension.

Wet foams have a structure similar to suspensions of soft spheres, at packing fractions slightly above the jamming point. When this limit is approached, bubble motions become more collective and their dynamics exhibit diverging characteristic length and time scales [9,10]. Neighboring bubbles are pushed against each other and deformed by the confinement pressure Π, also called osmotic pressure [11]. Recent experiments with wet foams and granular suspensions have shown in both cases that the steady flow rheology is governed by the product of the shear rate and the relaxation time η/Π, interpreted as the duration of a rearrangement (η is the suspending liquid viscosity) [12–14]. However, this prediction has so far not been confirmed by direct observations.

In this Letter, we investigate experimentally how the duration of coarsening-induced bubble rearrangements in 3D foams depends on osmotic pressure, liquid viscosity, and bubble size. The rearrangement dynamics are probed using time-resolved diffusing-wave spectroscopy (DWS), a multiple coherent light scattering technique [15–18]. A laser beam (wavelength $\lambda = 532$ nm) is focused by a lens on the surface of the foam. After a diffusive penetration into the sample, most of the light is backscattered. Some of this scattered light is collected by a multimode fiber near the focus. Its other end faces the sensor of a high speed CCD line camera where a speckle interference pattern is formed. This pattern fluctuates rapidly whenever a bubble rearrangement occurs in the part of the foam probed by the diffusive light paths. The space-time diagram shown in Fig. 1(a) illustrates these intermittent dynamics. To characterize the temporal fluctuations quantitatively we calculate the normalized autocorrelation function, which depends on time t and a delay time τ:

$$F(t,\tau) = \frac{2\langle I_t I_{t+\tau}\rangle - \langle I_t\rangle^2 - \langle I_{t+\tau}\rangle^2}{\langle I_t^2\rangle + \langle I_{t+\tau}^2\rangle - \langle I_t\rangle^2 - \langle I_{t+\tau}\rangle^2}. \quad (1)$$

I_t is the intensity detected at a given pixel of the camera at time t and the brackets denote an average over the pixels.

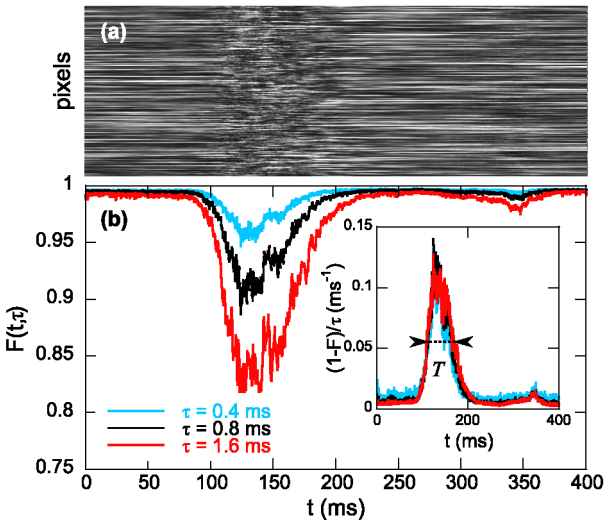

FIG. 1 (color online). (a) Space-time plot of the speckle pattern, obtained by the juxtaposition of the 1024 pixels (vertical axis) whose intensities are measured at successive instants t (horizontal axis). (b) Intensity correlation function $F(t,\tau)$ as a function of time t for different delays τ. Inset: $[1 - F(t,\tau)]/\tau$ as a function of t for the same delays τ. The arrows show the full width at half maximum of the peak.

In the absence of bubble motion $F \approx 1$, but when a rearrangement occurs in the scattering volume, F drops sharply [Fig. 1(b), see also Fig. S1 in the Supplemental Material [19]). In the case of random ballistic scatterer motion with average velocity v, the theory of DWS predicts $F(t, \tau) = \exp(-8\pi v\tau/\lambda)$ [16]. If $\tau \ll \lambda/(8\pi v)$, the correlation drop $1 - F$ should scale linearly with both v and τ. Our data follow indeed such a scaling with τ [inset, Fig. 1(b)], and we therefore use $[1 - F(t, \tau)]/\tau$ as a robust measure of bubble dynamics. The peaks of this signal indicate rearrangements whose duration is either determined as the full width at half maximum denoted T [inset, Fig. 1(b)] or deduced from the decay time of the 4th order temporal autocorrelation function $g_4(s, \tau) = \langle[1 - F(t, \tau)][1 - F(t + s, \tau)]\rangle_t$ (where $\langle\ldots\rangle_t$ is a time average). Both choices are found to give consistent results.

We use foaming solutions composed of a mixture of two surfactants: sodium lauryl-dioxyethylene sulfate (SLES from Stepan Co. USA, at concentration 0.33 wt%) and cocoamidopropyl betaine (CAPB from Goldschmitt, Germany, at concentration 0.17 wt%). These solutions are known to have low interfacial rigidity (mobile interfaces) [20]. To tune the bulk viscosity η from 1.6 to 9.7 mPa · s (at 23 °C) glycerol is added with a concentration G ranging from 20 to 60 wt%. The solution and nitrogen gas are injected into a microfluidic device [21] that generates monodisperse bubbles with a diameter d chosen in the range 120 to 240 μm. The foam is injected into a container where liquid drains and accumulates at the bottom until an equilibrium between gravity and capillary forces is reached. The foam structure is initially polycrystalline, but coarsening progressively introduces polydispersity and disorder [Fig. 2(a) and video S2 in the Supplemental Material [19]]. All measurements are conducted before this process creates a significant increase of the mean bubble diameter [Fig. 2(b)].

To investigate the influence of osmotic pressure Π, samples of different foam heights (from 1.5 to 30 mm) are made to float on the liquid. In the region near the top surface probed by the DWS measurements, the osmotic pressure is set by the buoyancy of the bubbles below [11]: $\Pi = \rho\Omega g/\Sigma$ (ρ denotes the liquid density, Ω the gas volume contained in the foam, estimated by weighing the container and by measuring the whole sample volume, and Σ the horizontal sample cross section). Therefore, tuning the sample height enables us to set Π near the top surface in the range 10–300 Pa. The pressure imposes the liquid fraction ε, depending on the foam structure. For a monodisperse crystalline foam, we have

$$\Pi = k\frac{\gamma}{d}\frac{(\varepsilon_c - \varepsilon)^\beta}{\sqrt{\varepsilon}}, \qquad (2)$$

where $\varepsilon_c = 0.26$ is the close packing fraction of a fcc structure, $k = 14.7$ and $\beta = 2$, up to liquid fractions close to ε_c [22]. Osmotic pressure in a disordered emulsion has

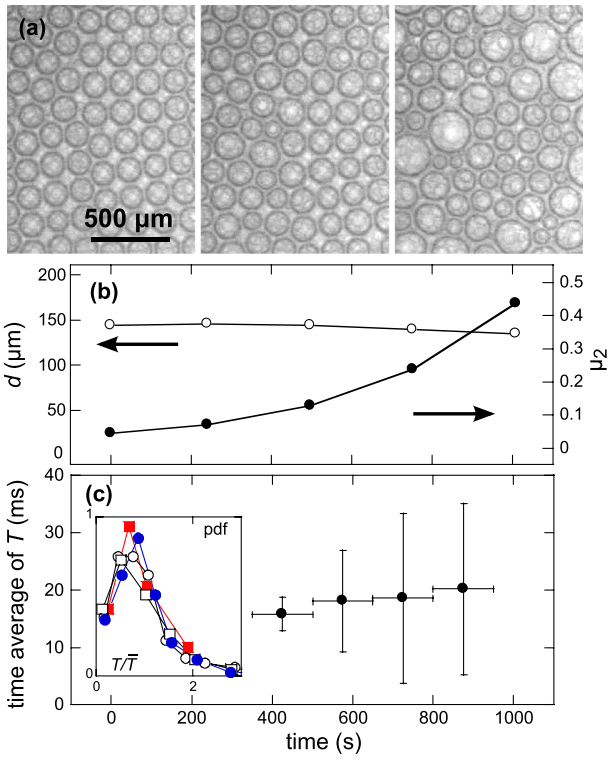

FIG. 2 (color online). (a) Photographs of the foam top surface at time 0, 500, and 1000 s after production ($G = 20\%$, $\Pi = 60$ Pa). (b) Time evolution of the average bubble diameter d (○) and the normalized standard deviation μ_2 (●). (c) Time average (over successive periods of 150 s) of the rearrangement duration T (see Fig. 1) vs time. The vertical error bars show the standard deviation. Inset: probability density function of the duration T normalized by the average duration $\bar{T}$ over one experiment for $\Pi = 9$ Pa (■), $\Pi = 23$ Pa (○), $\Pi = 60$ Pa (□), and $\Pi = 160$ Pa (●).

been measured, for liquid fractions up to 0.2 [11]. These data can be fitted by Eq. (2) with $\varepsilon_c = 0.36$ the close packing fraction of a disordered packing, $k = 7.0$ and $\beta = 2.5$. Note that these β values are not valid in the asymptotic limit $\varepsilon \to \varepsilon_c$. For $d = 100$ μm and $\gamma = 30$ mN/m, Eq. (2) shows that the pressure range in our experiments corresponds to liquid fractions $0.11 < \varepsilon < 0.23$ for crystalline foams ($0.08 < \varepsilon < 0.27$ for disordered foams). Moreover, the DWS backscattering measurement probes the foam on a typical depth $2.5l^*$, where l^* is the light transport mean free path [17]. For the liquid fraction values in our experiment, $l^*/d \approx 2$–3 [23], so that the optically probed volume is a fraction of millimeter in height.

Since the osmotic pressure and the bubble size are fixed, the transition from an ordered to a disordered structure as coarsening progresses is accompanied by a change in ε up to a factor 2 (for the driest samples). Remarkably, this change does not affect significantly the average rearrangement duration [Fig. 2(c)], indicating that Π rather than ε is the dominant control parameter for rearrangement dynamics. The standard deviation of T increases with disorder

(Fig. 2), possibly due to increasing event size fluctuations, but we have checked that the probability distribution of the normalized duration over an experiment is independent of Π [inset, Fig. 2(c)] so that the average duration $\bar{T}$ can be considered as a robust time scale.

Figure 3 shows $\bar{T}$ measured as a function of Π for different bubble diameters and glycerol contents. As the wet limit is approached, $\bar{T}$ increases roughly as Π^{-1}, over a decade in osmotic pressure. Moreover, $\bar{T}$ increases with bubble size or bulk viscosity. The average duration $\bar{T}$ cannot depend on long range structural correlations in the packing: otherwise, the passage from the monodisperse polycrystalline to the polydisperse disordered structure would have an impact on $\bar{T}$, in contrast with the data in Fig. 2(c). For this reason, we focus on a simple rearrangement mechanism neglecting correlations between bubble displacements.

Rearrangements in foams are reminiscent of those in steadily flowing hard spheres suspensions [12,14]. It was found that their constitutive law is governed by the characteristic duration of a structural rearrangement in the granular assembly [12]. The driving force that pushes a grain towards its new configuration scales as Πd^2. Its motion is hindered by the viscous resistance due to fluid displacement through the packing interstices [12]. As a grain moves a typical distance d, it displaces a liquid volume εd^3 through a porous medium of permeability αd^2 and is thus slowed down by a modified Stokes friction force $\eta(d^2/\bar{T})(\varepsilon/\alpha)$ which reflects the Darcy flow. Balancing the driving and friction forces yields the relaxation time

$$\bar{T} \sim \frac{\eta}{\Pi}\frac{\varepsilon}{\alpha}. \tag{3}$$

In contrast to solid grains, bubbles in wet foams are deformed if osmotic pressure is applied, so that thin, approximately flat liquid films are formed at the contacts between neighbors. If the gas-liquid interfaces are rigid, shear flow in these films is expected to be a significant mechanism of dissipation. However, for totally mobile interfaces, there cannot be any shear flow in the films and the dominant friction mechanism must be the viscous Darcy flow through the bubble packing, just as in the case of hard sphere suspensions. To check whether this picture is correct and whether Eq. (3) describes our data, we first recall that the permeability coefficient α has been measured for wet foams with mobile interfaces as a function of liquid fraction ε [24]. Using this empirical law and Eq. (2), the factor ε/α can be expressed as a function of the reduced osmotic pressure defined as $\tilde{\Pi} = \Pi/(\gamma/d)$. When we decrease $\tilde{\Pi}$ from 1 to 10^{-1} in our experiments, ε/α decreases by a factor up to 2.5, and it tends to a constant value of order 10^3 at the jamming point where $\tilde{\Pi} \to 0$. Finally, Eq. (3) can be rewritten in terms of the parameters that we control or measure experimentally:

$$\bar{T}\frac{\gamma}{\eta d} = A\frac{1}{\tilde{\Pi}}\frac{\varepsilon(\tilde{\Pi})}{\alpha(\tilde{\Pi})}. \tag{4}$$

A is a dimensionless prefactor. Since the parameters k, β, and ε_c in Eq. (2) depend on the packing structure, $\varepsilon(\tilde{\Pi})/\alpha(\tilde{\Pi})$ is slightly different for ordered and disordered foams. In Fig. 4, we compare our data obtained for different viscosities and bubble sizes to Eq. (4) and observe a good collapse onto the predicted master curve. The only fitted parameter is $A = 0.33$, which is of the order of 1, as expected.

Our results thus provide further evidence for the analogy between local relaxation dynamics in suspensions of solid grains and wet foams with mobile interfaces, both governed by the time scale $\eta\varepsilon/(\alpha\Pi)$. For a foam with rigid interfaces (Gillette foam), rearrangement durations have been reported to be 1 order of magnitude larger than those found in our experiments, for similar bubble size, liquid content, and liquid viscosity [6,17], indicating the presence

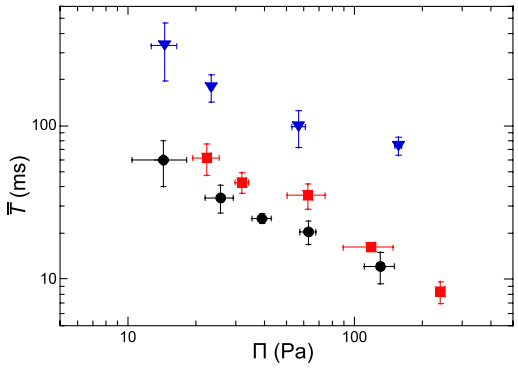

FIG. 3 (color online). Average rearrangement duration $\bar{T}$ as a function of the osmotic pressure Π, for different bubble diameters d and glycerol content G: (●) $d = 140$ μm, $G = 20$ wt % ($\gamma = 30$ mN/m); (■) $d = 240$ μm, $G = 20$ wt %; (▼) $d = 120$ μm, $G = 60$ wt % ($\gamma = 28$ mN/m). Each data point is an average over 2 to 10 different samples.

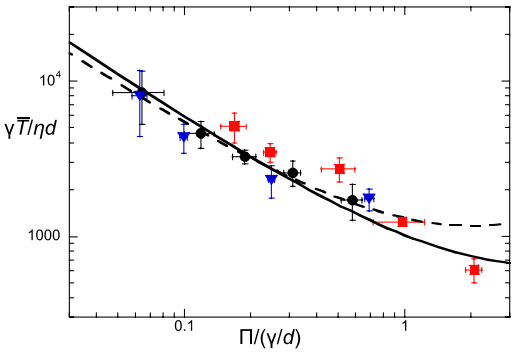

FIG. 4 (color online). Normalized duration $\gamma\bar{T}/(\eta d)$ as a function of the reduced osmotic pressure $\tilde{\Pi} = \Pi/(\gamma/d)$ (same symbols as in Fig. 3). The solid and dashed lines represent the prediction Eq. (4), respectively, for ordered and disordered foams. In both cases, the fitted parameter is $A = 0.33$.

of an additional dissipation mechanism. To achieve a full understanding of rearrangement dynamics in foams and similar complex fluids, it will therefore be necessary to investigate the impact of interfacial rigidity on the mechanism of dissipation.

We thank C. Caroli for stimulating discussions, E. Lorenceau for providing us the permeability values, J. Laurent and I. Muttoni for crucial help in setting up the experiment, and S. Costa for surface tension measurements. This work was supported by the European Space Agency (Contract No. MAP AO 99-108) and the French Space Agency (agreement CNES/CNRS No. 103954).

[1] D. Weaire and S. Hutzler, *The Physics of Foams* (Oxford University Press, Oxford, 1999).
[2] I. Cantat, S. Cohen-Addad, F. Elias, F. Graner, R. Höhler, O. Pitois, F. Rouyer, and A. Saint-Jalmes, *Les Mousses: Structure et Dynamique* (Belin, Paris, 2010).
[3] D. J. Durian, D. A. Weitz, and D. J. Pine, Science **252**, 686 (1991).
[4] S. Cohen-Addad, R. Höhler, and Y. Khidas, Phys. Rev. Lett. **93**, 028302 (2004).
[5] R. Höhler and S. Cohen-Addad, J. Phys. Condens. Matter **17**, R1041 (2005).
[6] A. Gopal and D. J. Durian, J. Colloid Interface Sci. **213**, 169 (1999).
[7] M. Durand and H. A. Stone, Phys. Rev. Lett. **97**, 226101 (2006).
[8] A.-L. Biance, S. Cohen-Addad, and R. Höhler, Soft Matter **5**, 4672 (2009).
[9] D. J. Durian, Phys. Rev. E **55**, 1739 (1997).
[10] T. Hatano, Phys. Rev. E **79**, 050301 (2009).
[11] H. M. Princen and A. D. Kiss, Langmuir **3**, 36 (1987).
[12] C. Cassar, M. Nicolas, and O. Pouliquen, Phys. Fluids **17**, 103301 (2005).
[13] F. Boyer, E. Guazzelli, and O. Pouliquen, Phys. Rev. Lett. **107**, 188301 (2011).
[14] R. Lespiat, S. Cohen-Addad, and R. Höhler, Phys. Rev. Lett. **106**, 148302 (2011).
[15] D. A. Weitz and D. J. Pine, *Dynamic Light Scattering*, edited by W. Brown (Clarendon, Oxford, 1993).
[16] P. K. Dixon and D. J. Durian, Phys. Rev. Lett. **90**, 184302 (2003).
[17] A. S. Gittings and D. J. Durian, Phys. Rev. E **78**, 066313 (2008).
[18] D. A. Sessoms, H. Bissig, A. Duri, L. Cipelletti, and V. Trappe, Soft Matter **6**, 3030 (2010).
[19] See Supplemental Material at http://link.aps.org/supplemental/10.1103/PhysRevLett.108.188301 for a figure showing the autocorrelation function F for several rearrangements and a movie of a foam sample at the first stages of coarsening.
[20] K. Golemanov, N. D. Denkov, S. Tcholakova, M. Vethamuthu, and A. Lips, Langmuir **24**, 9956 (2008).
[21] E. Lorenceau, Y. Yip Cheung Sang, R. Höhler, and S. Cohen-Addad, Phys. Fluids **18**, 097103 (2006).
[22] R. Höhler, Y. Yip Cheung Sang, E. Lorenceau, and S. Cohen-Addad, Langmuir **24**, 418 (2008).
[23] M. U. Vera, A. Saint-Jalmes, and D. J. Durian, Appl. Opt. **40**, 4210 (2001).
[24] E. Lorenceau, N. Louvet, F. Rouyer, and O. Pitois, Eur. Phys. J. E **28**, 293 (2009).